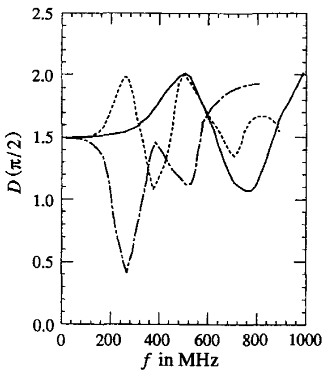

Fig. 6. Horizontal directivity $D(\pi/2)$ for a biconical antenna in free space. Solid line: $h = 6$ in., $a = 10$ in.; dash-dotted line: $h = 6$ in., $a = 20$ in.; dotted line: $h = 12$ in., $a = 20$ in.

finite ground plane will, of course, distort these patterns.) As seen in Fig. 5, the curves for variously sized bicones are quite similar with respect to the variations in the radiation pattern. At low frequencies when the antenna is electrically small, the pattern is similar to that of a short dipole [4] which is circular or oval in shape and in three dimensions has the appearance of a toroid (i.e., "doughnut"-shaped). The maximum radiation occurs at $\Theta = \pi/2$. At the higher frequencies where the exit aperture is of the order of a wavelength or larger, the maximum radiation moves away from the horizontal direction and minor lobes appear. As a consequence, the horizontal directivity can decrease at higher frequencies, especially for the larger size bicones.

Directivity curves have also been computed. The directivity in the direction Θ_m, $D(\Theta_m)$, is the ratio of the integral of the Poynting vector with the value of the electric field at $\Theta = \Theta_m$ to the actual value of the integral, or

$$D(\Theta_m) = \frac{\int_0^{2\pi} \int_0^{\pi} E^*(\Theta_m)E(\Theta_m)\sin\Theta\, d\Theta\, d\Phi}{\displaystyle\int_0^{2\pi} \int_0^{\pi} E^*(\Theta)E(\Theta)\sin\Theta\, d\Theta\, d\Phi}. \tag{7}$$

After the Φ-integrations, (7) reduces to

$$D(\Theta_m) = \frac{2|E(\Theta_m)|^2}{\int_0^{\pi} E^*(\Theta)E(\Theta)\sin\Theta\, d\Theta}. \tag{8}$$

When the antenna is electrically short, $D(\Theta_m) = 3/2$ which is the result for an infinitesimal dipole.

Horizontal directivity curves are shown in Fig. 6. Note that with the larger bicones there are frequencies at which the horizontal directivity is drastically reduced. On the other hand, a small bicone with $h = 3$ in., $a = 5$ in. (not shown) does not suffer from this effect and actually has values of $D(\pi/2)$ that increase with frequency.

V. CONCLUSION

A broadband omnidirectional antenna for use on a vehicle is described and analyzed. The associated far-field patterns including the effect of earth or sea are derived in [1].

ACKNOWLEDGMENT

The authors are pleased to acknowledge the graphics and computational assistance of Barbara H. Sandler and the editorial assistance of Margaret Owens.

REFERENCES

[1] R. W. P. King and S. S. Sandler, "The electromagnetic field of a vertical electric dipole over the earth or sea," *IEEE Trans. Antenn. Propagat.*, vol. 42, no. 3, Mar. 1994, pp. 382–389

[2] C. H. Papas and R. W. P. King, "Input impedance of wide-angle conical antennas fed by a coaxial line," *Proc. IRE*, vol. 37, no. 11, pp. 1269–1271, Nov. 1949.

[3] C. H. Papas and R. W. P. King, "Radiation from wide-angle conical antennas fed by a coaxial line," *Proc. IRE*, vol. 39, no. 1, pp. 49–51, Jan. 1951.

[4] R. W. P. King, R. B. Mack and S. S. Sandler, *Arrays of Cylindrical Dipoles*, Cambridge Univ. Press, New York, 1968, pp. 11–14.

A New Formulation for the Design of Chebyshev Arrays

Ahmad Safaai-Jazi

***Abstract*—A new formulation for the design of Chebyshev arrays is presented which makes no direct use of Chebyshev polynomials. The array factor is expressed in terms of cosine/cosine-hyperbolic functions based on which all analysis and design steps are carried out. Zeros of the array factor are used to obtain a system of equations for excitation currents. Solving this system of equations, current magnitudes are determined in terms of the current of one element chosen as the independent variable. A general formulation for even or odd but otherwise arbitrary number of elements is presented. The minimum number of elements required to achieve the desired beamwidth and side lobe level is obtained in a single step without resorting to an iterative process. The optimum spacing between elements for broadside and end fire arrays is also addressed. Numerical results for example cases are provided.**

I. INTRODUCTION

Chebyshev arrays have the unique property that all side lobes in their radiation pattern are of equal magnitude [1]. Traditionally, the analysis and design of Chebyshev arrays have been carried out with the help of Chebyshev polynomials [2]–[4]. The process involves expressing the array factor as a polynomial whose coefficients are in terms of element current magnitudes. This polynomial is then compared with a Chebyshev polynomial of the same order and coefficients of like power terms are equated. A linear system of equations then results which is solved for current magnitudes in terms of the current of one element chosen as the independent variable. This approach, while useful in illuminating the fundamental aspects of Chebyshev arrays, becomes quite involved when the number of elements is large.

In this article, a new approach to the design of Chebyshev arrays is presented which allows for a unified formulation to be readily obtained for an arbitrary number of elements. The key point in this approach is that no direct use is made of Chebyshev polynomials.

Manuscript received May 18, 1993; revised September 22, 1993.
The author is with the Bradley Department of Electrical Engineering, Virginia Polytechnic Institute and State University, Blacksburg, VA 24061.
IEEE Log Number 9215670.

Instead, the array factor is expressed in terms of cosine/cosine-hyperbolic functions which serve as alternative representations to Chebyshev polynomials [5]. Zeros of the array factor are easily determined from the cosine function representation. Using these zeros, a system of equations for element current magnitudes is then readily obtained. The solution of this system of equations is presented in a matrix form for even or odd but otherwise arbitrary number of elements. Zeros of the array factor have been used before in a different formulation of the Chebyshev array [6]. However, this formulation, which uses a polynomial representation of the array factor, is not general and becomes quite involved for large number of elements.

In a design problem with unknown number of elements but specified side lobe level and beamwidth, the common practice has been to determine the minimum number of elements required to meet the design specifications through a trial and error procedure. Here, an equation is derived from which the minimum number of elements is obtained in a single step without resorting to an iterative process, hence a considerably more efficient design approach.

Two cases corresponding to even and odd number of elements are considered. It is assumed that among side lobe level, half-power beamwidth, and number of elements, two quantities are specified and the third quantity as well as excitation currents (relative to the current of one element considered as an independent variable) are sought. Both broadside and endfire arrays are examined. Formulae for optimum spacing between the elements are given and numerical results for example design cases are also presented.

II. Array Factor

Let us consider a linear array of N equally spaced elements with nonuniform excitations. Assuming a symmetrical distribution for magnitude of currents and a constant inter-element phase shift α, the array factor for even and odd number of elements can be expressed as

$$f(\psi) = 2\sum_{m=1}^{n} I_m \cos\left[\left(m-\frac{1}{2}\right)\psi\right], \quad N = 2n, \tag{1a}$$

and

$$f(\psi) = I_o + 2\sum_{m=1}^{n} I_m \cos(m\psi), \quad N = 2n+1, \tag{1b}$$

where $\psi = \beta d\cos\theta + \alpha, \beta = 2\pi/\lambda; \lambda$ being the wavelength, d is the element spacing, θ is the angle measured from the line of array, I_m is the magnitude of current for the mth element on either side of the array midpoint, and I_o denotes the current of the center element when N is odd.

Taking advantage of the fact that Chebyshev polynomials satisfy the relationships $T_n(\cos x) = \cos(nx)$ for $|T_n| < 1$ and $T_n \cos(hx) = \cos h(nx)$for $T_n \geq 1$, the array factor in (1a) or (1b) is written as

$$|f(\psi)| = |f(\overline{\psi})| = \begin{cases} C\left|\cos\left[\frac{(N-1)}{2}\overline{\psi}\right]\right|, & |f(\psi)| \leq C, \quad (2a) \\ C\cos h\left[\frac{N-1}{2}\overline{\psi}\right], & |f(\psi)| \geq C, \quad (2b) \end{cases}$$

where C is a positive constant coefficient and the relationship between ψ and $\overline{\psi}$ is given by

$$\gamma\cos\left(\frac{\psi}{2}\right) = \begin{cases} \cos(\frac{\overline{\psi}}{2}), & |f(\psi)| \leq C, (3a) \\ \cos h(\frac{\overline{\psi}}{2}), & |f(\psi)| \geq C. (3b) \end{cases}$$

In (3a) and (3b), γ is a real coefficient which can be determined when design specifications are known. It is evident from (1a) and (1b) that $f(\psi)$ assumes its maximum value at $\psi = 0$. This corresponds to $\overline{\psi} = \overline{\psi}_o = 2\cos h^{-1}(\gamma)$. Let us, for the time being, assume that the number of elements N and beam maximum-to-side lobe level ratio R (side lobe level in dB is - $20\log R$) are specified. Since all side lobes are of the same magnitude C as implied by equation (2a), the ratio R satisfies the relation

$$R = \cos h\left[\frac{(N-1)}{2}\overline{\psi}_o\right] = \cos h[(N-1)\cos h^{-1}(\gamma)]. \tag{4}$$

Solving (4) for γ, yields

$$\gamma = \cos h\left[\frac{1}{(N-1)}\ln(R+\sqrt{R^2-1})\right]. \tag{5}$$

Calculation of γ when N and half-power beamwidth HPBW or R and HPBW are given will be discussed later. The coefficient C if the array factor is required to be normalized to unity is determined as $C = 1/R$.

III. Calculation of Excitation Currents

Zeros of the array factor are used to establish the system of equations governing current magnitudes. These zeros are solutions of $\cos\left[(N-1)\overline{\psi}/2\right] = 0$, which yields $\overline{\psi} = [(4m \pm 1)\pi]/(N-1)$ with m being an integer. Due to the symmetry of the array factor about $\overline{\psi} = \pi$, it suffices to consider only the zeros in the range $0 < \overline{\psi} < \pi$. It can be shown that such zeros are obtained from

$$\overline{\psi}_m = \frac{(2m-1)\pi}{N-1}, m = 1, 2, \ldots, M, \tag{6}$$

where $M = (N-2)/2$ for N even and $M = (N-1)/2$ for N odd. Using (3a), the zeros in terms of ψ are given by

$$\psi_m = 2\cos^{-1}\left[\frac{1}{\gamma}\cos\left(\frac{(2m-1)\pi}{2(N-1)}\right)\right], \quad m = 1, 2, \ldots, M. \tag{7}$$

On the other hand, ψ_m are zeros of $f(\psi)$ in (1a) or (1b); that is,

$$f(\psi_m) = 0, m = 1, 2, \ldots, M. \tag{8}$$

(8) is, in fact, a system of M equations and $M+1$ unknowns. The unknowns are current magnitudes I_m, one of which is chosen as an independent variable. For even number of elements, I_{M+1} is chosen as the independent variable. The remaining M currents are then obtained from the following matrix equation,

$$\begin{bmatrix} I_1 \\ I_2 \\ \vdots \\ I_M \end{bmatrix} = -I_{M+1}[A]^{-1}\begin{bmatrix} \cos[(M+\frac{1}{2})\psi_1] \\ \cos[(M+\frac{1}{2})\psi_2] \\ \vdots \\ \cos[(M+\frac{1}{2})\psi_m] \end{bmatrix}, \tag{9}$$

where

$$[A] = \begin{bmatrix} \cos(\frac{\psi_1}{2}) & \cos(\frac{3\psi_1}{2}) & \cdots & \cos[(2M-1)\frac{\psi_1}{2}] \\ \cos(\frac{\psi_2}{2}) & \cos(\frac{3\psi_2}{2}) & \cdots & \cos[(2M-1)\frac{\psi_2}{2}] \\ \vdots & \vdots & & \vdots \\ \cos(\frac{\psi_M}{2}) & \cos(\frac{3\psi_M}{2}) & \cdots & \cos[(2M-1)\frac{\psi_M}{2}] \end{bmatrix}. \tag{10}$$

For odd number of elements, I_o is chosen as the independent variable. The remaining M currents are then obtained from

$$\begin{bmatrix} I_1 \\ I_2 \\ \vdots \\ I_M \end{bmatrix} = -\frac{1}{2}I_o[B]^{-1}\begin{bmatrix} 1 \\ 1 \\ \vdots \\ 1 \end{bmatrix}, \tag{11}$$

where

$$[B] = \begin{bmatrix} \cos\psi_1 & \cos(2\psi_1) & \cdots & \cos(M\psi_1) \\ \cos\psi_2 & \cos(2\psi_2) & \cdots & \cos(M\psi_2) \\ \vdots & \vdots & \vdots & \vdots \\ \cos\psi_M & \cos(2\psi_M) & \cdots & \cos(M\psi_M) \end{bmatrix}. \tag{12}$$

IV. Relationship Among Beamwidth, Side Lobe Level and Number of Elements

Let us assume that $\theta = \theta_h$ corresponds to a half-power point on the main beam of the array pattern. For broadside array ($\alpha = 0$) there exist two half-power points, on the left and right sides of $\theta = \pi/2$. Considering $\theta_h < \pi/2$, the half-power beamwidth for broadside arrays is HPBW $= \pi - 2\theta_h$. For endfire arrays ($\alpha = \pm\beta d$), there exists only one solution for θ_h(here $d \leq d_{\rm opt}$ is assumed, see Eq. (20)), and HPBW $= \theta_h$ when $\alpha = -\beta d$, while HPBW$= (\pi - \theta)$ for $\alpha = \beta d$. Without loss of generality, endfire arrays with $\alpha = -\beta d$ are considered in the following analysis. For endfire arrays with $d = \lambda/2$, $\theta_h =$ HPBW/2. Let $\psi = \psi_h$ at $\theta = \theta_h$, then $\psi_h = \beta d \cos\theta_h$ for broadside case , and $\psi_h = \beta d(\cos\theta_h - 1)$ for endfire case. From (3b)

$$\overline{\psi}_h = 2\cos h^{-1}\Big(\gamma\cos\Big(\frac{\psi_h}{2}\Big)\Big). \tag{13}$$

Recalling that at $\overline{\psi} = \overline{\psi}_o$ the array factor assumes its maximum value, from (2b), (4), (5), and (13) it follows that

$$\cos(\frac{\psi_h}{2})\cos h\Big[\frac{1}{N-1}\cos h^{-1}(R)\Big] - \cos h\Big[\frac{1}{N-1}\cos h^{-1}(\frac{\sqrt{2}}{2}R)\Big] = 0. \tag{14}$$

Equation (14) is a relationship among half-power beamwidth, side lobe level, and the number of elements. Thus, if two of these three quantities are specified the third one can be determined from (14). The case when R and N are given has already been studied. The beamwidth, in this case, is obtained from

$$\text{HPBW} = \begin{cases} \pi - 2\cos^{-1}(\frac{\psi_h}{\beta d}), & \text{broadside}, \quad (15a) \\ \cos^{-1}(1 + \frac{\psi_h}{\beta d}), & \text{endfire}, \quad (15b) \end{cases}$$

where

$$\psi_h = 2\cos^{-1}\left\{\frac{\cos h\Big[\frac{1}{N-1}\cos h^{-1}(R/\sqrt{2})\Big]}{\cos h\Big[\frac{1}{N-1}\cos h^{-1}(R)\Big]}\right\}. \tag{16}$$

For endfire arrays with $d = \lambda/2$, the right-hand side of (15b) is multiplied by 2.

For the case when N and HPBW (and thus ψ_h) are known, (14) may be solved for the unknown R. Clearly, (14) is a transcendental equation whose solution for R should be sought numerically. Having found R, excitation currents are readily determined using the formulation outlined in Section III.

Finally, if R and HPBW are given, (14) may be again solved numerically for N. This solution denoted as N_0 is generally non-integer, whereas N must be an integer number. Therefore, the minimum number of elements required to achieve half-power beamwidth and side lobe level equal to or smaller than the specified values is determined from

$$N = \text{ integer part of } N_0 + 1. \tag{17}$$

The above discussions and results are applicable to both even and odd number of elements.

V. Optimum Spacing

The spacing d may be optimized such that for a specified side lobe level and given number of elements the smallest possible beamwidth is achieved. This amounts to accommodating as many side lobes as possible in the radiation pattern of the array. In doing so, the visible range in the $\overline{\psi}$ domain, corresponding to the range $0 \leq \theta \leq \pi$, is so determined to include all side lobes on both sides of the main beam in broadside arrays, and on one side of it in endfire arrays, as well as a portion of the grating lobe which will produce a side lobe with a magnitude equal to the specified side lobe level. The cutoff point on the grating lobe should satisfy the relation

$$\cos h\Big[\frac{(N-1)}{2}\overline{\psi}\Big] = \Big|\cos\Big[\frac{(N-1)}{2}\overline{\psi}\Big]\Big|, \tag{18}$$

which is possible only if $\overline{\psi} = 0$. The value of ψ corresponding to $\overline{\psi} = 0$ can be obtained from (3a). It should, however, be noted that in (3a), $0 \leq \psi \leq \pi$ is presumed. Thus, the solution $\psi = 2\cos^{-1}(1/\gamma)$ has to be discarded, because this corresponds to a point on the main beam at which $\overline{\psi} = 0$. The solution of ψ corresponding to grating lobe lies in the range $\pi < \psi < 2\pi$. However, in this range $\cos\frac{\psi}{2} < 0$ and (3a) should be modified as $-\gamma\cos(\psi/2) = \cos(\overline{\psi}/2)$. Putting $\overline{\psi} = 0$ in this equation, $\psi = 2\pi - 2\cos^{-1}(1/\gamma)$ is obtained.

For broadside arrays, ψ should correspond to $\theta = 0$, that is $\psi = \beta d_{\rm opt}$, resulting in

$$d_{\rm opt} = \lambda\Big[1 - \frac{\cos^{-1}(1/\gamma)}{\pi}\Big], \quad \text{broadside}. \tag{19}$$

For endfire arrays with the main beam in the $\theta = \pi$ direction, ψ should correspond to $\theta = 0$, that is $\psi = 2\beta d_{\rm opt}$, resulting in

$$d_{\rm opt} = \frac{\lambda}{2}\Big[1 - \frac{\cos^{-1}(1/\gamma)}{\pi}\Big], \quad \text{endfire}. \tag{20}$$

Obviously (20) is also valid for endfire arrays with the main beam in the $\theta = 0$ ($\alpha = -\beta_d$) direction. Optimization of spacing d for endfire arrays with $\alpha \neq \pm\beta d$ is also possible. This case has been addressed elsewhere [7].

The minimum number of elements with optimum spacing when beamwidth and side lobe level are specified still can be obtained from (14) provided that d is substituted by $d_{\rm opt}$ in (19) and (20).

TABLE I
Current Magnitudes for Linear Equally Spaced Chebyshev Arrays. Currents of Edge Elements are Unity.

N	SLL (dB)	-10	-20	-30	-40
3		1.0390	1.6364	1.8774	1.9604
4		0.8794	1.7357	2.3309	2.6688
5		0.7905	1.9319	3.1397	4.1480
		0.7248	1.6085	2.4123	3.0131
6		0.6808	1.8499	3.3828	4.9891
		0.6071	1.4369	2.3129	3.0853
7		0.6102	1.8387	3.7846	6.2731
		0.5864	1.6837	3.3071	5.2678
		0.5191	1.2764	2.1507	3.0071
8		0.5413	1.7244	3.8136	6.8448
		0.5103	1.5091	3.0965	5.1982
		0.4519	1.1386	1.9783	2.8605
9		0.4923	1.6627	3.9565	7.6989
		0.4813	1.5800	3.6516	6.9168
		0.4494	1.3503	2.8462	4.9516
		0.3995	1.0231	1.8158	2.6901
10		0.4463	1.5585	3.8830	7.9837
		0.4306	1.4360	3.4095	6.6982
		0.4003	1.2125	2.5986	4.6319
		0.3576	0.9264	1.6695	2.5182

VI. Numerical Results

For given number of elements N and side lobe level SLL, current magnitudes are calculated by first finding ψ_m from (7) and then solving (9) if N is even or (11) if N is odd. Currents are normalized such that the current of edge elements is unity; i.e., $I_n = 1$. Currents of the remaining elements of the array; namely, I_1, I_2,..., I_{n-1}, when N is even ($= 2n$) and I_0, I_1, I_2, ..., I_{n-1} when N is odd ($= 2n + 1$) are summarized in Table I for $N = 3, 4, \ldots, 10$ and SLL

TABLE II
HALF-POWER BEAMWIDTH IN DEGREES FOR BROADSIDE CHEBYSHEV ARRAYS. FOR EACH VALUE OF N, THE FIRST AND SECOND ROWS CORRESPOND TO $d = \lambda/2$ AND $d = d_{\text{opt}}$, RESPECTIVELY.

N	SLL (dB)	-10	-20	-30	-40
3		36.45	40.38	41.92	42.45
		24.27	31.28	35.95	38.80
4		25.61	30.08	32.57	33.81
		15.58	20.62	24.66	27.69
5		19.61	23.71	26.40	28.04
		11.36	15.11	18.33	20.98
6		15.84	19.46	22.06	23.82
		8.91	11.83	14.42	16.66
7		13.27	16.45	18.87	20.62
		7.32	9.69	11.82	13.71
8		11.42	14.23	16.44	18.12
		6.21	8.19	9.99	11.60
9		10.01	12.53	14.55	16.13
		5.39	7.08	8.63	10.02
10		8.91	11.19	13.04	14.52
		4.76	6.24	7.58	8.81

TABLE III
HALF-POWER BEAMWIDTH IN DEGREES FOR ENDFIRE CHEBYSHEV ARRAYS. FOR EACH VALUE OF N THE FIRST AND SECOND ROWS CORRESPOND TO $d = \lambda/2$ AND $d = d_{\text{opt}}$, RESPECTIVELY.

N	SLL (dB)	-10	-20	-30	-40
3		93.17	98.19	100.08	100.72
		54.58	62.55	67.49	70.38
4		77.78	84.45	87.96	89.66
		43.20	50.06	55.04	58.56
5		67.86	74.77	79.00	81.47
		36.68	42.51	47.04	50.51
6		60.87	67.59	72.06	74.95
		32.37	37.45	41.50	44.74
7		55.64	62.06	66.54	69.62
		29.27	33.78	37.44	40.42
8		51.54	57.65	62.04	65.18
		26.91	30.99	34.31	37.07
9		48.22	54.04	58.30	61.44
		25.04	28.78	31.83	34.38
10		45.47	51.01	55.13	58.23
		23.51	26.97	29.80	32.18

$= -10, -20, -30$, and -40 dB. For the sake of brevity, the edge element currents, which all are equal to unity, are omitted from the table. With the help of this table, currents of all elements are readily available. For example, for $N = 7$ and SLL $= -20$ dB the current are: 1, 1.2764, 1.6837, 1.8387, 1.6837, 1.2764, 1.

The corresponding half-power beamwidths for broadside and endfire arrays are presented in Tables II and III. The results for beamwidth are calculated using (15) and (16). In these two tables, there are two entries for each SLL-N combination. The first entry is the half-power beamwidth corresponding to element spacing $d = \lambda/2$, while the second entry is that for $d = d_{\text{opt}}$ as specified in (19) and (20). As an example, for a broadside array with $N = 9$ and SLL $= -30$ dB, the half-power beamwidth is 14.55° if $d = \lambda/2$ and 8.63° if $d = d_{\text{opt}} = 0.8419\lambda$. The optimum spacings for the broadside case are given in Table IV. The optimum spacings for the endfire case ($\alpha = \pm\beta d$) are one-half of those for the broadside array. Part of the results in Table I are available elsewhere [7]. They have been produced here primarily for the purpose of comparison and checking the correctness of the proposed method.

A. Design Example

An endfire array with side lobe level of -20 dB and half-power beamwidth of 22.50° is to be designed. Determine the minimum

TABLE IV
OPTIMUM SPACING IN TERMS OF WAVELENGTH FOR BROADSIDE ARRAY.

N	SLL (dB)	-10	-20	-30	-40
3		0.7438	0.6402	0.5796	0.5449
4		0.8179	0.7249	0.6566	0.6078
5		0.8600	0.7814	0.7170	0.6655
6		0.8867	0.8199	0.7619	0.7124
7		0.9050	0.8474	0.7957	0.7496
8		0.9182	0.8679	0.8216	0.7792
9		0.9283	0.8836	0.8419	0.8031
10		0.9361	0.8960	0.8583	0.8226

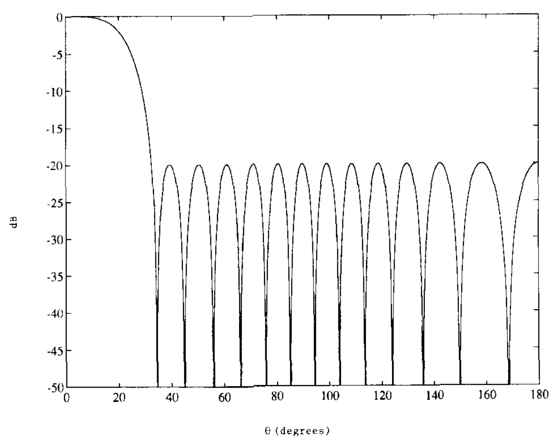

Fig. 1. Radiation pattern of an endfire Chebyshev array with 14 elements and element spacing $d = 0.4636\lambda$. The side lobe level is-20 dB and the half-power beamwidth is 22.10°.

number of elements, the excitation currents, and the optimum spacing.
Step 1 From $R = 10^{-\text{SLL}/20}$, $R = 10$ is calculated. Then, with $\theta_h = 22.5°$ and combining (5), (14), and (20), we have an equation in which only N is unknown. Solving this equation numerically, $N = N_o = 13.596$ is obtained. However, since N must be an integer and in order to have HPBW $\leq 22.5°$, according to (17) $N = 14$ is considered.
Step 2 For $N = 14$ and $R = 10$ from (5) and (7) γ and ψ_m, $m = 1, 2, \ldots 6$ are determined, respectively. Then, assuming $I_7 = 1$, equation (9) is solved with the following results: $I_1 = 1.2684$, $I_2 = 1.2190$, $I_3 = 1.1245$, $I_4 = 0.9931$, $I_5 = 0.8359$, and $I_6 = 0.6655$. Finally, from (20) the optimum spacing $d_{\text{opt}} = 0.4636\lambda$ is obtained.

To ensure that the design meets the specified requirement, the half-power beamwidth is examined. From (15b) for $N = 14$, $R = 10$, and $d = 0.4636\lambda$, we obtain HPBW $= 22.10°$ which is slightly less than maximum required beamwidth of 22.5°. $N = 14$ should be the minimum number of elements. This is indeed the case, because for $N = 13$ and $R = 10$ the smallest achievable beamwidth is calculated to be 23.06° which exceeds the maximum beamwidth of 22.5°. A plot of the radiation pattern for this endfire array is shown in Figure 1.

VII. CONCLUSION

A unified formulation for Chebyshev arrays with arbitrary number of elements has been presented. This formulation is sufficiently general, lends itself to simple computer-aided design algorithms, and allows for quick analysis of Chebyshev arrays. Design parameters can be obtained without the need for a trial and error process. An equation in terms of the number of elements, side lobe level, and half-power beamwidth has been derived which facilitates the design process considerably.

Acknowledgment

The author would like to thank Y. Kim for performing the computations.

References

[1] C. L. Dolph, "A current distribution for broadside arrays which optimizes the relationship between beamwidth and side lobe level," *Proc. IRE,* vol. 34, 1946, pp. 335–348.
[2] W. L. Weeks, *Antenna Engineering,* New York, McGraw-Hill, 1968, ch. 3.
[3] W. L. Stutzman and G. A. Thiele, *Antenna Theory and Design,* John Wiley and Sons, 1981, ch. 10.
[4] R. E. Collin, *Antennas and Radiowave Propagation,* New York, McGraw-Hill, 1985, ch. 3.
[5] I. S. Gradshteyn and I. M. Ryzhik, *Table of Integrals, Series and Products,* New York, Academic Press, 1965.
[6] K. F. Lee, *Principles of Antenna Theory,* New York, John Wiley and Sons, 1984, ch. 7.
[7] R. C. Johnson and H. Jasik, *Antenna Engineering Handbook,* New York, McGraw-Hill, 1984, ch. 3.

Comments on "An Improved Pulse-Basis Conjugate Gradient FFT Method for the Thin Conducting Plate Problem"

A. Peter M. Zwamborn

In the above cited paper,[1] Tran and McCowen present pulse-basis expansion functions and Dirac δ testing functions within a conjugate gradient FFT (CGFFT) formulation. In the conclusions, they state: "Although these spurious effects do not appear in the CGFFT formulation using the rooftop basis function proposed by Zwamborn and van den Berg [1], there are more computational costs associated with their method than with ours." At this point, I strongly disagree with this statement.

Close examination of (3) reveals that the method proposed by Tran and McCowen uses four scalar convolutions to be evaluated for each operator computation. The weak form of the conjugate gradient FFT (WCGFFT) method introduced by Zwamborn and van den Berg [1] needs only two scalar convolutions. Since these convolutions consume a dominant part of the computation of the operator, it is straightforwardly observed that the WCGFFT method needs significantly less CPU time per iteration. Further, we remark that Tran and McCowen have left out the numerical convergence rate of the WCGFFT method while comparing their method with other CGFFT methods. Therefore, we present in Fig. 1 the numerical convergence rates of all various schemes. This figure is composed by copying Fig. 2 of the above paper,[1] but now including the WCGFFT results from [1, Fig. 1]. From the present figure, it is shown that the WCGFFT method converges within far fewer iterations than Tran and McCowen's CGFFT method. As mentioned in [1] in the last paragraph of Section IV, a considerable decrease of computation time is achieved by using the discrete cyclic convolution (see also [2]). For example, in the case where we have discretized the plate into 31 subdomains, the CPU time per WCGFFT iteration on a VAX6400 minicomputer amounts to 2.5 s instead of 10 s for the spectral representation that is presented in [1].

Further, Tran and McCowen claim in the conclusions that: "The extraneous ripples which are formed in the interior of the induced surface densities in our method do not significantly affect the overall quality of the current distributions.... Yet, there is little compromise in accuracy, particularly in the far field..." To discuss this statement in more detail, we consider the results of the circular disk as

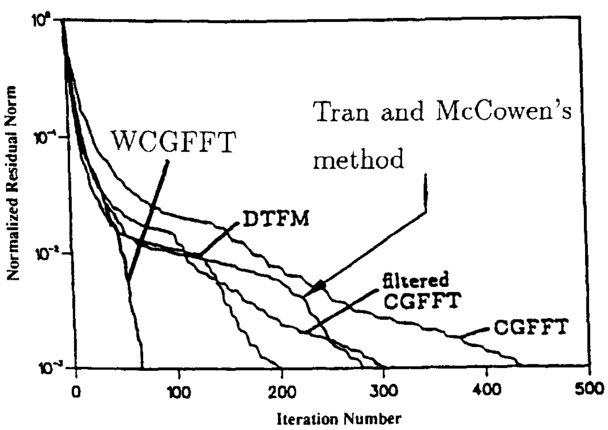

(a)

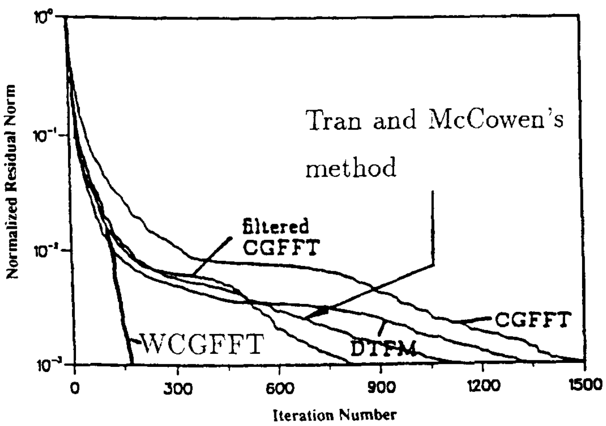

(b)

Fig. 1. (a) The obtained numerical convergence rate of a $\lambda \times \lambda$ plate with normal incidence for $\Delta x = \Delta y = \lambda/17$. (b) The obtained numerical convergence rate of a $\lambda \times \lambda$ plate with normal incidence for $\Delta x = \Delta y = \lambda/33$.

Manuscript received August 4, 1993.

The author is with the Electromagnetic Effects Group, TNO Physics and Electronics Laboratory, Oude Waalsdorperweg 63, 2509 JG The Hague, The Netherlands.

IEEE Log Number 9215668.

[1] T. V. Tran and A. McCowen, *IEEE Trans. Antenn. Propagat.,* vol. 41, pp. 185–190, Feb. 1993.